

EMI Two-Probe Scanning Short Term Scientific Mission (STSM)

Johannes A. Russer

Institute for Nanoelectronics, Technische Universität München, Arcisstrasse 21, 80333 Munich, Germany

Host: Dave Thomas

GGIEMR, University of Nottingham



The University of
Nottingham

UNITED KINGDOM · CHINA · MALAYSIA



COST IC 1407 Meeting and Training Session
at the University of Nottingham
April 4th-6th, 2016

Outline

- 1 Introduction
- 2 Scalar Stochastic Fields
- 3 Near-Field Scanning
- 4 Principal Component Analysis
- 5 Correlation Measurements and Experimental Setup
- 6 Conclusion

Outline

- 1** Introduction
- 2 Scalar Stochastic Fields
- 3 Near-Field Scanning
- 4 Principal Component Analysis
- 5 Correlation Measurements and Experimental Setup
- 6 Conclusion

Introduction

- Noise in electromagnetic fields and radiated electromagnetic interference (EMI) are ubiquitous limiting factors for the performance of wireless communication and electromagnetic sensor systems.
- Due to the equivalence principle, an equivalent source distribution determined by amplitude and phase scanning of the tangential electric or magnetic field on a surface enclosing the radiating structure is equivalent to the internal sources and allows the modeling of the environmental field.
- Due to the lack of information about the sources of the radiated EMI, the near field to be measured has to be treated as a stochastic field.

Introduction

- The modeling of stochastic fields differs from the modeling of deterministic fields since we have to consider the correlation between any pair of field samples.
- A methodology for the numerical computation of noisy electromagnetic fields excited by spatially distributed noise sources with arbitrary spatial correlation is discussed.
 - J. A. Russer and P. Russer, "Modeling of noisy EM field propagation using correlation information," *IEEE Transactions on Microwave Theory and Techniques*, vol. 63, no. 1, pp. 76–89, Jan. 2015
- Two-probe measurements are discussed.

Introduction

- RF circuits and high bit-rate digital circuits radiate EMI.
- This noise is mainly excited by switching operations in digital circuitry.
- This noise has to be treated as stochastic noise due to lack of knowledge.
- For optimum EMI compliant design of circuits an accurate modeling of the influence of EMI on circuits is required.

Outline

- 1 Introduction
- 2 Scalar Stochastic Fields**
- 3 Near-Field Scanning
- 4 Principal Component Analysis
- 5 Correlation Measurements and Experimental Setup
- 6 Conclusion

Scalar Stochastic Fields

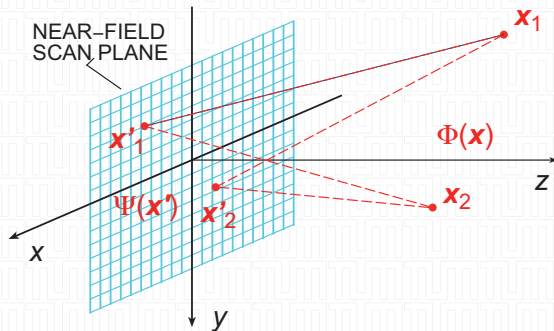
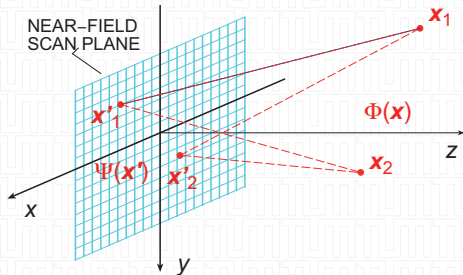


Figure: Near and far field.

The aperture field $\Psi(x')$ is the source of a far-field $\Phi(x)$.

Near and Far Field



The far-field $\Phi(\mathbf{x}, \omega)$ is related to the near-field $\Psi(\mathbf{x}', \omega)$ via

$$\Phi(\mathbf{x}, \omega) = \int_A G_0(\mathbf{x}, \mathbf{x}', \omega) \Psi(\mathbf{x}', \omega) d^3 \mathbf{x}', \quad (1)$$

where the *scalar Green's function* $G_0(\mathbf{x}, \mathbf{x}')$ is given by

$$G_0(\mathbf{x}, \mathbf{x}', \omega) = \frac{\exp[-jk(\mathbf{x} - \mathbf{x}')]}{|\mathbf{x} - \mathbf{x}'|}. \quad (2)$$

Stochastic Scalar Fields

$$c_{\phi}(\mathbf{x}_1, \mathbf{x}_2, \tau) = \lim_{T \rightarrow \infty} \frac{1}{2T} \int_{-\infty}^{\infty} \phi_T(\mathbf{x}_1, t) \phi_T(\mathbf{x}_2, t - \tau) dt. \quad (3)$$

- s_T denotes the *time-windowed field*, defined by

$$\phi_T(\mathbf{x}_1, t) = \begin{cases} \phi(\mathbf{x}_1, t) & \text{for } -T < t < T \\ 0 & \text{for } |t| \geq T \end{cases}. \quad (4)$$

- The Fourier transform of $c_{\phi}(\mathbf{x}_1, \mathbf{x}_2, \tau)$ is the *correlation spectrum*

$$\Gamma_{\phi}(\mathbf{x}_1, \mathbf{x}_2, \omega) = \int_{-\infty}^{\infty} c_{\phi}(\mathbf{x}_1, \mathbf{x}_2, \tau) \exp(-j\omega\tau) d\tau. \quad (5)$$

Stochastic Scalar Fields

- We can also obtain the correlation spectra directly from the spectra $\Phi_T(\mathbf{x}, \omega)$ of the time-windowed fields by

$$\Gamma_\phi(\mathbf{x}_1, \mathbf{x}_2, \omega) = \lim_{T \rightarrow \infty} \frac{1}{2T} \langle \Phi_T(\mathbf{x}_1, \omega) \Phi_T^*(\mathbf{x}_2, \omega) \rangle, \quad (6)$$

where the brackets denote the forming of the *ensemble average*.

Stochastic Scalar Fields

- To express the correlation spectrum of the far-field $\Gamma_\phi(\mathbf{x}_1, \mathbf{x}_2, \omega)$ as a function of the *correlation spectrum of the near-field*, given by

$$\Gamma_\psi(\mathbf{x}_1, \mathbf{x}_2, \omega) = \lim_{T \rightarrow \infty} \frac{1}{2T} \langle \Psi_T(\mathbf{x}_1, \omega) \Psi_T^*(\mathbf{x}_2, \omega) \rangle, \quad (7)$$

we insert (1) into (6) and obtain

$$\begin{aligned} \Gamma_\phi(\mathbf{x}_1, \mathbf{x}_2) &= \lim_{T \rightarrow \infty} \frac{1}{2T} \iint_A G_0(\mathbf{x}_1, \mathbf{x}'_1) \\ &\quad \times \langle \Phi_T(\mathbf{x}'_1) \Phi_T^*(\mathbf{x}'_2) \rangle G_0^*(\mathbf{x}_2, \mathbf{x}'_2) d^3 x'_1 d^3 x'_2 \\ &= \iint_A G_0(\mathbf{x}_1, \mathbf{x}'_1) \Gamma_\psi(\mathbf{x}'_1, \mathbf{x}'_2) G_0^*(\mathbf{x}_2, \mathbf{x}'_2) d^3 x'_1 d^3 x'_2. \end{aligned} \quad (8)$$

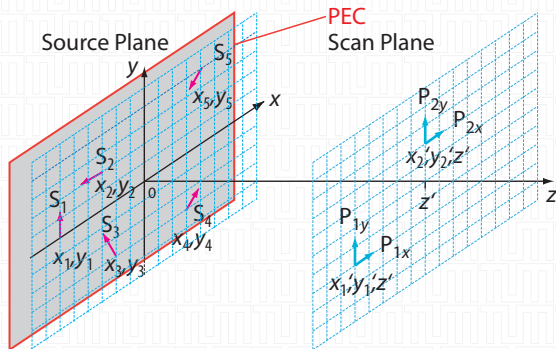
Stochastic Scalar Fields

- This allows to compute the *field correlation spectrum* $\Gamma_\phi(\mathbf{x}_1, \mathbf{x}_2)$ for the field amplitudes at the points of observation \mathbf{x}_1 and \mathbf{x}_2 from the correlation spectrum of the source field $\Gamma_\psi(\mathbf{x}'_1, \mathbf{x}'_2)$.
- *To compute the field excited by a distribution of stochastic sources requires not only the knowledge of the spatial distribution of the spectral energy density of the source but also the full information about the cross correlation of the source field amplitudes at any pair of points \mathbf{x}'_1 and \mathbf{x}'_2 .*

Outline

- 1 Introduction
- 2 Scalar Stochastic Fields
- 3 Near-Field Scanning**
- 4 Principal Component Analysis
- 5 Correlation Measurements and Experimental Setup
- 6 Conclusion

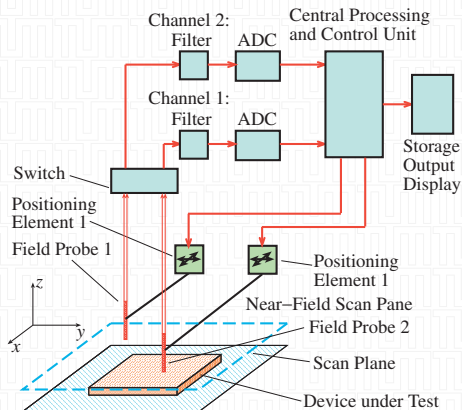
Near-Field Distribution of Sources in a Plane



Planar array of 5 sources sampled at a plane parallel to the source plane.

- J. A. Russer and P. Russer, "Modeling of noisy EM field propagation using correlation information," *IEEE Transactions on Microwave Theory and Techniques*, vol. 63, no. 1, pp. 76–89, Jan. 2015
- J. A. Russer, F. Mukhtar, O. Filonik, G. Scarpa, and P. Russer, "Modelling of noisy EM field propagation using correlation information of sampled data," in *IEEE Int. Conf. on Numerical Electromagnetical Modeling and Optimization NEMO2014*, Pavia, Italia, May 2014

Near-Field Distribution of Sources in a Plane



Schematic drawing of the near-field scanning system.

Computation of the Near-Field

Accounting also for the near-field contributions the Green's dyadic is given by

$$\mathbf{G}(\mathbf{x}, \omega) = [g_1(\mathbf{x}, \omega)\mathbf{1} + g_2(\mathbf{x}, \omega)\mathbf{x}\mathbf{x}^T] e^{-j\beta(\omega)|\mathbf{x}|}. \quad (9)$$

- $\mathbf{1}$: identity matrix
- $|\mathbf{x}| = \sqrt{x^2 + y^2 + z^2}$
- $\beta = \omega/c_0$: phase coefficient
- c_0 : free-space light velocity

$$g_1(\mathbf{x}, \beta) = -\frac{jZ_{F0}\beta^2}{4\pi} \left[\frac{1}{\beta|\mathbf{x}|} + \frac{j}{\beta^2|\mathbf{x}|^2} - \frac{1}{\beta^3|\mathbf{x}|^3} \right], \quad (10a)$$

$$g_2(\mathbf{x}, \beta) = \frac{jZ_{F0}\beta^2}{4\pi} \left[\frac{1}{\beta|\mathbf{x}|^3} + \frac{3j}{\beta^2|\mathbf{x}|^4} - \frac{3}{\beta^3|\mathbf{x}|^5} \right]. \quad (10b)$$

$Z_{F0} = \sqrt{\epsilon_0/\mu_0}$ is the free space wave impedance, and the T denotes the transpose of the vector.

- J. A. Russer and P. Russer, "Modeling of noisy EM field propagation using correlation information," *IEEE Transactions on Microwave Theory and Techniques*, vol. 63, no. 1, pp. 76–89, Jan. 2015

Near-Field Distribution of Sources in a Plane

$S_1 \dots S_5$ sources arranged in plane $z = 0$ at positions $\mathbf{x}_\nu = [x_\nu, y_\nu, 0]^T$, $\nu = 1 \dots N$.

Assumption: ν^{th} dipole has an impressed current $I_{T,\nu}(\omega)$, an infinitesimal length l_ν and an angular orientation characterized by the azimuth and pole angles φ_ν and ϑ_ν .

Current density $\mathbf{J}_\nu(\mathbf{x}, \omega)$ of the ν^{th} dipole given by

$$\mathbf{J}_T(\mathbf{x}, \omega) = \sum_{\nu=1}^N l_\nu I_{T,\nu}(\omega) \boldsymbol{\Omega}_\nu \delta(\mathbf{x} - \mathbf{x}_\nu). \quad (11)$$

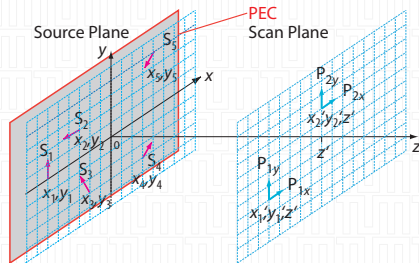
Angular orientation of the ν^{th} dipole described by normalized orientation vector

$$\boldsymbol{\Omega}_\nu = \begin{bmatrix} \sin \vartheta_\nu \cos \varphi_\nu \\ \sin \vartheta_\nu \sin \varphi_\nu \\ \cos \vartheta_\nu \end{bmatrix}, \quad (12)$$

$$\Gamma_J(\mathbf{x}_a, \mathbf{x}_b, \omega) = \sum_{\mu=1}^N \sum_{\nu=1}^N l_\mu l_\nu C_{I,\mu\nu}(\omega) \boldsymbol{\Omega}_\mu \boldsymbol{\Omega}_\nu^T \delta(\mathbf{x}_a - \mathbf{x}_\mu) \delta(\mathbf{x}_b - \mathbf{x}_\nu) \quad (13)$$

Near-Field Scanning (1)

- The orientation of the dipoles is parallel to the $x - y$ plane such that $\theta_\nu = \pi/2$ for all dipoles.
- For the dipoles in the plane $z = 0$ we chose equal lengths $l_\nu = 1\text{mm}$ and the positions $\mathbf{x}_1 = [-60, 0, 0]^T \text{mm}$, $\mathbf{x}_2 = [-30, 20, 0]^T \text{mm}$, $\mathbf{x}_3 = [-20, -30, 0]^T \text{mm}$, $\mathbf{x}_4 = [30, -30, 0]^T \text{mm}$, $\mathbf{x}_5 = [50, 40, 0]^T \text{mm}$, and the orientations $\varphi_1 = \pi/2$, $\varphi_2 = \pi$, $\varphi_3 = 2\pi/3$, $\varphi_4 = \pi/3$, and $\varphi_5 = 4\pi/3$.
- We assume uncorrelated excitation currents with the correlation matrix elements $C_{mn}^I = 10^{-6} \text{A}^2 \text{s}^{-1} \delta_{mn}$.



Near-Field Scanning (2)

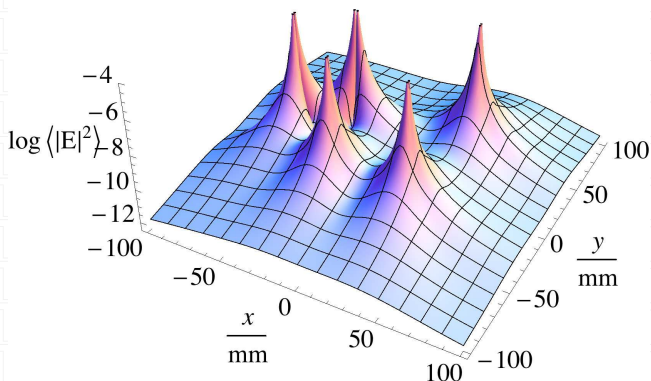
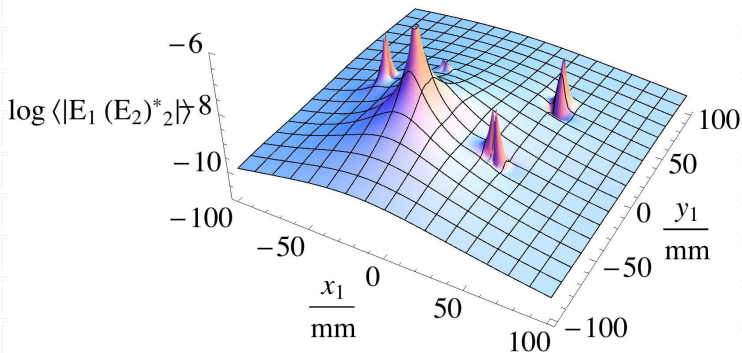


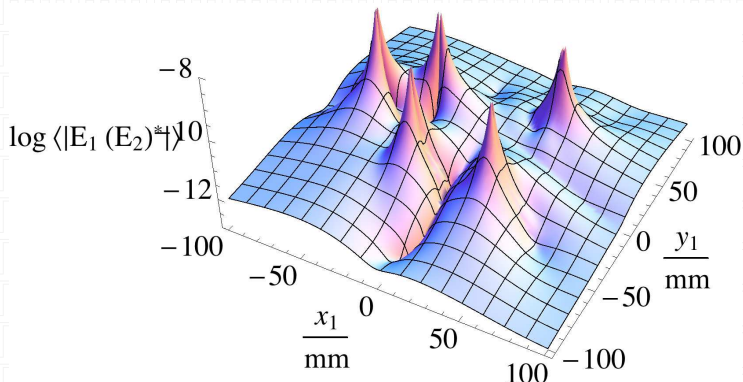
Figure: 3D logarithmic plot of the spectral electric energy density $|\Gamma_E(x, x, \omega)|$.

Near-Field Scanning (3)



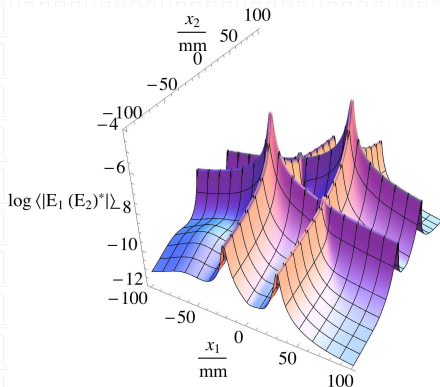
3D logarithmic plot of the magnitude of electric field correlation density $\Gamma_E(\mathbf{x}_1, \mathbf{x}_2, \omega)$, where probe 1 with the coordinates $[x'_1, y'_1, 1 \text{ mm}]^T$ scans over the area $\{-100 \text{ mm}, 100 \text{ mm}\}$ whereas the reference probe 2 is positioned at the fixed point $\mathbf{x}'_2 = [-20, -30, 1]^T \text{ mm}$ just over the source S_3 at \mathbf{x}_3 .

Near-Field Scanning (4)

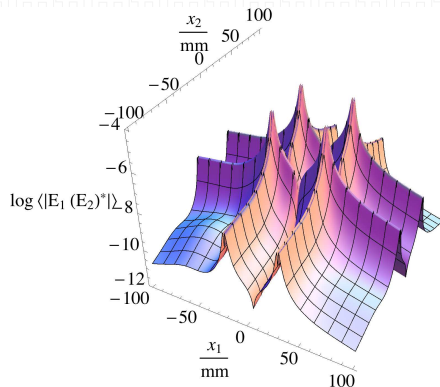


3D logarithmic plot of the magnitude of the electric field correlation density $\Gamma_E(\mathbf{x}_1, \mathbf{x}_2, \omega)$ for $x'_1, y'_1 \in \{-100 \text{ mm}, 100 \text{ mm}\}$, $z' = 1 \text{ mm}$, fixed reference point $\mathbf{x}'_2 = [-100, -100, 1]^T \text{ mm}$, and $\beta = 0.1 \text{ mm}^{-1}$.

Near-Field Scanning (5)



Uncorrelated sources



Correlated sources

3D logarithmic plot of $|\Gamma_E(x_1, x_2, \omega)|$, x_1 and x_2 varied independently, $z' = 1 \text{ mm}$, $y_1 = y_2 = -30 \text{ mm}$, and $\beta = 0.1 \text{ mm}^{-1}$.

Outline

- 1 Introduction
- 2 Scalar Stochastic Fields
- 3 Near-Field Scanning
- 4 Principal Component Analysis**
- 5 Correlation Measurements and Experimental Setup
- 6 Conclusion

Principal Component Analysis

- Principal Component Analysis (PCA) allows for reduction of the dimensionality of a multivariate data set without loss of information as well as for the identification of the principal directions in which the data are varying.
 - Each Principal Component (PC) represents a linear combination of data at specific coordinates (variables) at different values of a chosen parameter (called observations).
 - Computation of PCs is based on calculating the eigenvectors and eigenvalues (λ) of the data covariance matrix or correlation matrix.
 - The determination of eigenvectors is an iterative process and the eigenvectors are ranked by the eigenvalue, highest to lowest obtaining the PCs in order of significance.
- L. R. Arnaut, C. S. Obiekezie, and D. W. P. Thomas, "Empirical emission eigenmodes of printed circuit boards," *IEEE Transactions on Electromagnetic Compatibility*, vol. 56, no. 3, pp. 715–725, Jun. 2014
 - J. A. Russer, T. Asenov, and P. Russer, "Modeling of noisy electromagnetic fields using principal component analysis," in *Proc. European Microwave Conference (EuMC)*, Rome, Italy: IEEE, Oct. 2014, pp. 1099–1102

Criteria for determining the number of retainable PCs

- Several criteria have been proposed for determining a suitable number of PCs to account for most of the variance in a data set.
- A cumulative percentage of total variation rule in most of the cases recommends that the selected PCs should contribute more than 90% of total variance.
- In particular case one dominant PC can be retained if it contributes more than 70% of total variance.
- If the total number of the PCs is k than the explained variance that j -th PC accounts for is given as

$$\text{explained variance}(j) = 100 \frac{\lambda_j}{\sum_{i=1}^k \lambda_i} \%$$

- J. A. Russer, T. Asenov, and P. Russer, "Modeling of noisy electromagnetic fields using principal component analysis," in *Proc. European Microwave Conference (EuMC)*, Rome, Italy: IEEE, Oct. 2014, pp. 1099–1102

Outline

- 1 Introduction
- 2 Scalar Stochastic Fields
- 3 Near-Field Scanning
- 4 Principal Component Analysis
- 5 Correlation Measurements and Experimental Setup**
- 6 Conclusion

Correlation Measurements and Experimental Setup

- Two-probe scanning in time domain is performed using a multi-channel digital oscilloscope and an automated setup for positioning of the probes.
- Scanning was performed on a linear array of measurement points with up to $N = 50$ measurement points. This yields a total of $N(N - 1)/2 = 1225$ pairs of measurement points.

DC Motors as Noise Source

- Small electric DC motors were used as EM noise sources. The motors are powered by a 9V DC supply provided through batteries.
- The contacts to the slip-rings, that rotate with the shaft, are provided by brushes and get frequently disrupted causing sparks. This gives rise to EM noise at high frequencies.

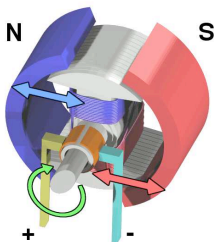


Figure: DC motor (from Wikipedia, https://en.wikipedia.org/wiki/DC_motor#/media/File:Electric_motor_cycle_2.png).

//en.wikipedia.org/wiki/DC_motor#/media/File:Electric_motor_cycle_2.png

DC Motors as Noise Source

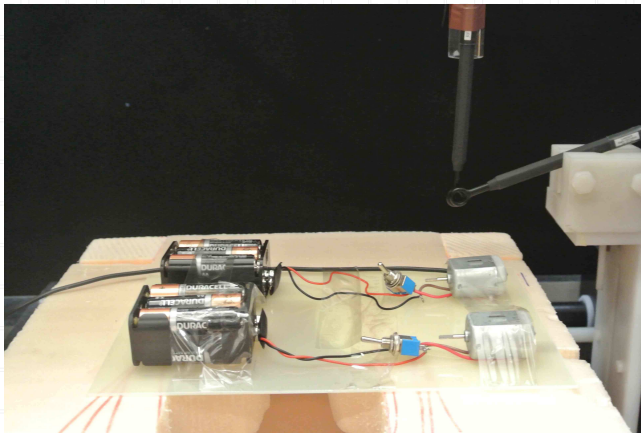


Figure: DC motors mounted on PCB.

DC Motors as Noise Source

- To get information on the typical noise emission spectrum, the electric motor was placed in a GTEM cell connected to a spectrum analyzer.
- The emission spectrum graphed in Fig. 5 shows strong emission at several hundreds of MHz and even up to 1.5GHz.

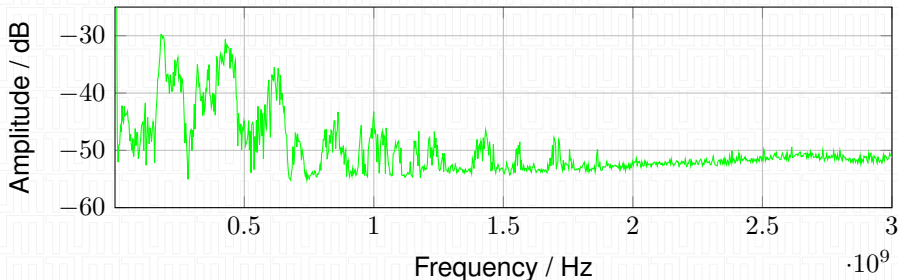


Figure: Noise emission spectrum of a single motor.

Experimental Setup

- About one million sample points were captured per channel for each measurement pair. The tangential magnetic field was sampled using a digital oscilloscope up to 1 GHz.
- Measurement setup included three motors mounted on an FR4 board and radiating into free space with probes located 4 cm above the motors, and a setup with nine motors mounted on an FR4 board and placed in a metallic box with a 5 mm wide and 23 cm long slit.

Probes and Slitted Box

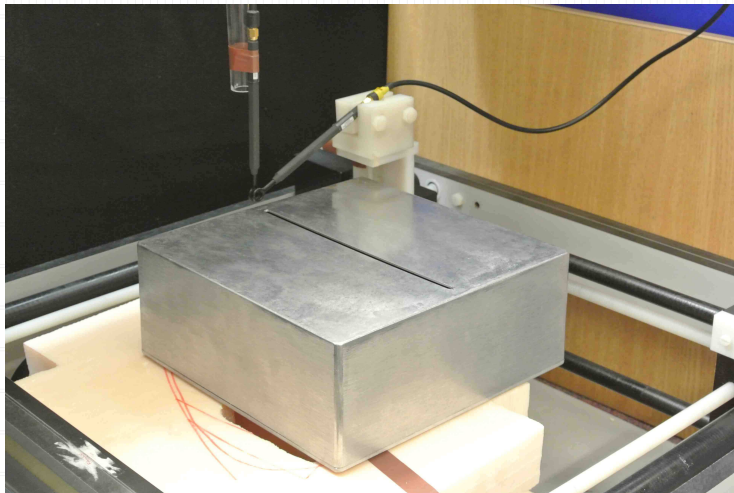


Figure: *Two-probe scanning arrangement for slitted box containing 9 electric motors serving as uncorrelated noise sources.*

Data Acquisition

- 50 spatial sampling points yield 1250 measurement position pairs for a single polarization.
- Measurement time up to 8hrs
- Yields \sim 30GB of data for a snapshot with one million sample points.

Fairly large amount of data has to be accounted for in analysis tools.

Data Analysis - Spectral Energy Density - Example 1

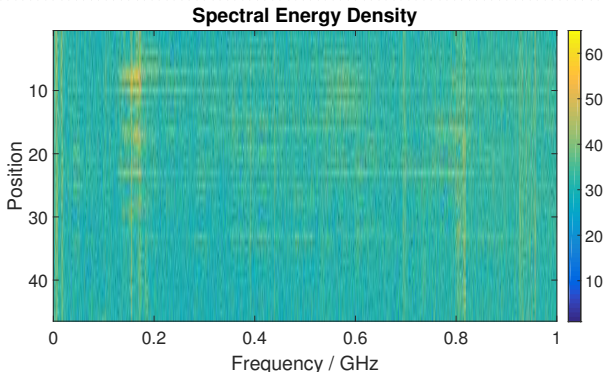


Figure: *Normalized spectral energy density as function of frequency and position along the scanning line.*

- J. A. Russer, M. Haider, M. H. Baharuddin, C. Smartt, A. Baev, S. Wane, D. Bajon, Y. Kuznetsov, D. Thomas, and P. Russer, "Correlation measurement and evaluation of stochastic electromagnetic fields," in *To be published at the EMC Europe 2016, Wroclaw, 2016*

Data Analysis - Correlation Matrices

Analysis of these measurement data yielded 46-by-46 correlation matrices.

Correlation Matrix Visualization (f=159.9112MHz)

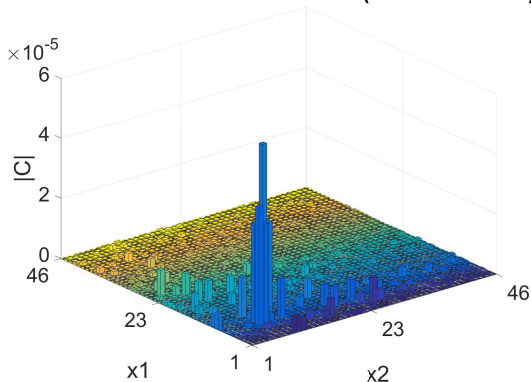


Figure: *Graphic representation of the absolute values of the correlation matrix at 159.9 MHz for setup with 3 motors.*

Data Analysis - Correlation Matrices

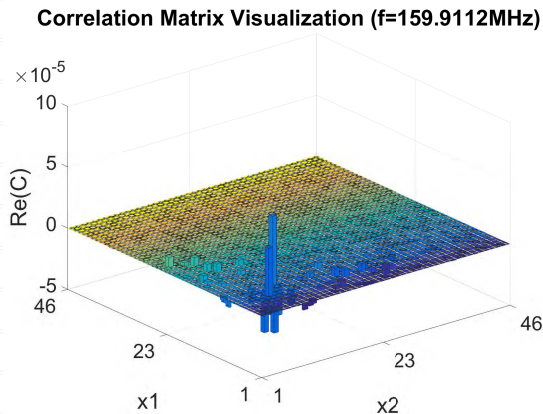


Figure: *Graphic representation of the real values of the correlation matrix at 159.9 MHz for setup with 3 motors.*

Data Analysis - Correlation Matrices

Correlation Matrix Visualization (f=159.9112MHz)

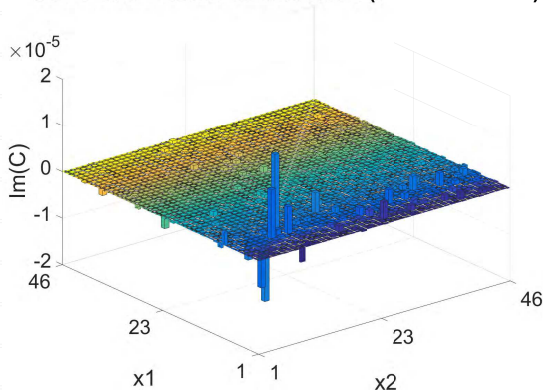


Figure: *Graphic representation of the imaginary values of the correlation matrix at 159.9 MHz for setup with 3 motors.*

Data Analysis - PCA

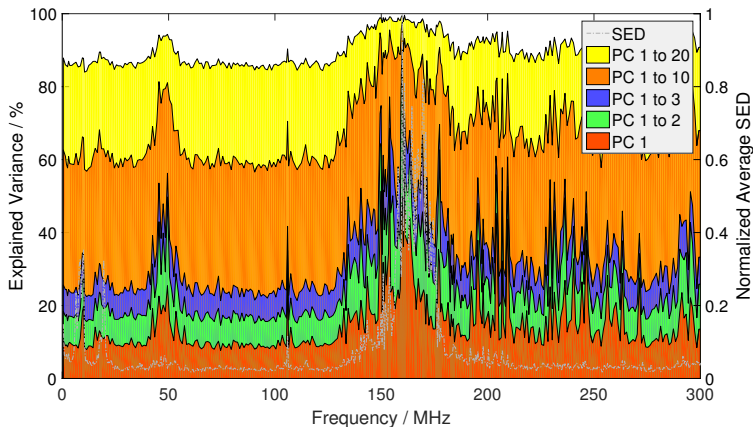


Figure: Cumulative explained variance of the principal component vs. frequency and spectral energy density.

Data Analysis - Example 2

Now, we consider the case of nine motors enclosed in a slitted box and the field is sampled above the 23 cm long slit at 50 positions with two probes at all possible pairs. A graphic visualization of the correlation matrix obtained for this setup at 9.4 MHz is shown in Figs. 12 and 13. The emissions are spatially more uniformly distributed over the observation points as can be seen from the contributions to the autocorrelation values in the diagonal of the matrix.

Data Analysis - Correlation Matrices

Analysis of these measurement data yielded 46-by-46 correlation matrices.

Correlation Matrix Visualization (f=9.9936MHz)

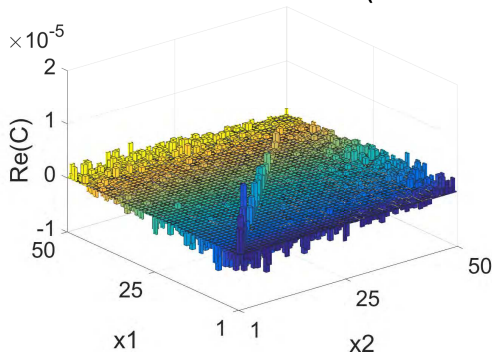


Figure: Graphic representation of the real values of the correlation matrix at 9.4 MHz for setup with 9 motors.

Data Analysis - Correlation Matrices

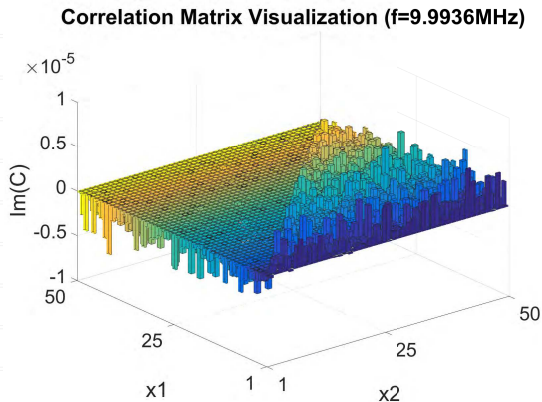


Figure: Graphic representation of the real values of the correlation matrix at 9.4 MHz for setup with 9 motors.

Data Analysis - PCA

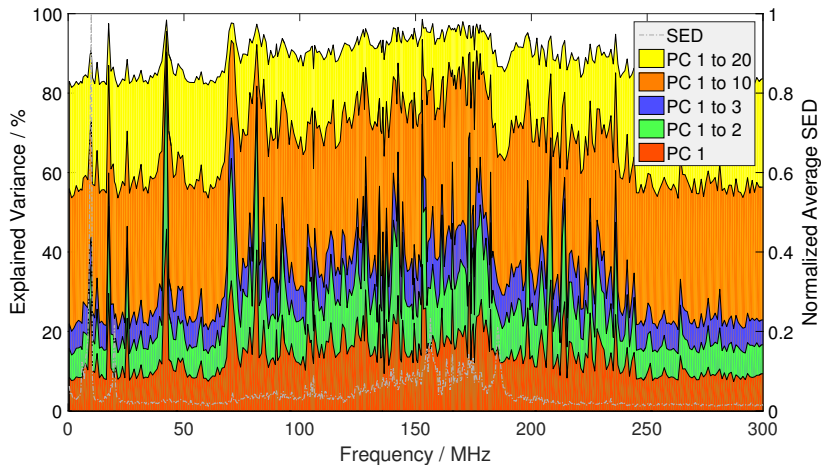


Figure: Cumulative explained variance of the principal component vs. frequency and spectral energy density.

Outline

- 1 Introduction
- 2 Scalar Stochastic Fields
- 3 Near-Field Scanning
- 4 Principal Component Analysis
- 5 Correlation Measurements and Experimental Setup
- 6 Conclusion

Conclusion

- For computation of the response to stochastic field excitation the response functions computed for deterministic fields can be used.
- For the correct modeling of stochastic electromagnetic fields the spatial correlations of the source distributions have to be considered.
- The measurement effort is feasible if modern time-domain EMI measurement systems are applied. The intensity and mutual correlation of noise sources can be analyzed.
- Eigenvalue decomposition and the PCA method considerably reduce the computational effort for computing the environmental field from the field sampled by identifying and retaining only the relevant variables without loss of information.

Acknowledgment

This short term scientific mission was facilitated by the COST Action “Advanced Characterisation and Classification of Radiated Emissions in Densely Integrated Technologies” (ACCREDIT) – IC1407, supported by COST (European Cooperation in Science and Technology).

I would like to thank

- Prof. Dave Thomas for hosting this mission,
- Mohd Hafiz Baharuddin, MSc,
- Dr. Chris Smartt, and
- the GGIEMR research group !

THANK YOU FOR YOUR KIND ATTENTION!